Advances in Science and Technology Research Journal

Advances in Science and Technology Research Journal, 2027, 21(1), 350–360
https://doi.org/10.12913/22998624/235871
ISSN 2299-8624, License CC-BY 4.0

Received: 2026.05.20
Accepted: 2026.11.15
Published: 2026.12.01

Thermo-elastohydrodynamic analysis of oil film characteristics in spiroid gear worm-wheel meshing

Aleksander Mazurkow[1], Wojciech Homik[2*]

[1] Faculty of Mechanical Engineering and Aeronautics, Rzeszow University of Technology, al. Powstanców Warszawy 12, 35-959 Rzeszow, Poland
* Corresponding author's e-mail: whomik@prz.edu.pl

ABSTRACT

The durability and reliability of mechanical gear transmissions, which also include spiroid gears, depend significantly on, among other factors, the lubrication parameters of the transmission. This type of transmissions is currently used in the drive systems of various types of vehicles. Under high loads, the aforementioned gear transmissions exhibit increased contact pressures on the meshing tooth surfaces. This results in the lubricant being "squeezed" out of the working space between the teeth, thereby increasing friction. This undesirable effect can be eliminated by generating an elastohydrodynamic (EHD) oil film in the working space between the meshing gear teeth. To determine the minimum oil film thickness, the isothermal model developed by Dowson is used, where the oil viscosity is given at ambient temperature and pressure. In reality, the oil temperature during gear operation deviates from the assumptions made in Dowson's model. In view of the above, in order to account for real operating conditions in the oil film, oil film thickness correction factors are used that consider the effect of temperature on oil viscosity. Accurate determination of the value of the oil film thickness correction factor is a complex issue; therefore, with the aim of providing the best possible approximation of the actual operating conditions of a spiroid gear, the authors proposed a new approach to this problem. The developed method utilizes oil characteristics, with properties such as viscosity and density determined experimentally. The gear operating parameters were determined by assuming oil temperature as a prescribed value in the computational model, corresponding to the actual temperature occurring in the meshing parts of the gear: the disc wheel and the worm. The computational model used to determine the oil film thickness also accounts for the materials used, the load-carrying capacity of the oil film and the oil flow velocity. The developed method is universal and can also be implemented for calculating other types of gear transmissions.

Keywords: spiroid gear, mechanical transmissions, elastohydrodynamic oil film.

INTRODUCTION

Spiroid gear transmissions are designs with special applications. Despite their compact size and significant speed reduction, they are capable of transmitting high torques. They also enable precise positioning of driven devices. They exhibit high resistance to overloads as well as high reliability and durability. These gears are used in electric motor vehicles, construction machinery, military vehicles as well as in aviation and astronautics [1–7].

The basic assembly in the gear design consists of a worm and a disc wheel (Figure 1). This assembly, together with bearings, is mounted in a housing. Spiroid gears are lubricated with gear oils. A detailed description of the construction of a transmission gear and the results of bench tests are presented in [8–12].

Despite their relatively simple design, spiroid gears pose a significant challenge for designers. One of the problems they encounter in the gear design process is the selection of the thermophysical properties of oil. This problem stems from high loads on the toothed rims combined with low oil flow velocities in their contact zone. During the operation of a spiroid gear, the following

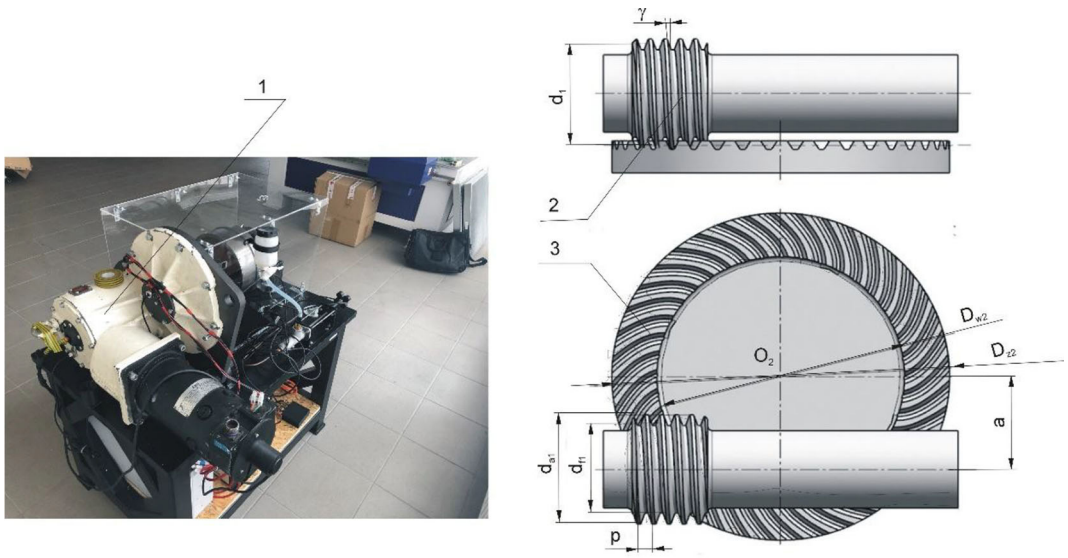


Figure 1. a) Test bench: 1 – spiroid gear, b) basic gear assembly: 2 – worm, 3 – disc wheel. Designations of geometric quantities: d_1 – pitch diameter of the worm, d_{a1} – outer diameter of the worm, d_{f1} – worm core diameter, γ – helix angle of the worm's thread line, D_{z2} – outer diameter of the disc wheel, D_{w2} – inner diameter of the disc wheel, a – distance from the worm axis to the center of the disc wheel, p – worm pitch

types of friction occur: static, boundary, mixed and fluid friction. As is well known, the most adverse conditions for interactions between the mechanical parts of a gear transmission occur during transient states, e.g. during startup, when the coefficient of friction *f* changes its value. The variation of the friction coefficient *f*(*He*) during gear startup is shown in Figure 2. For ω = 0, the Hersey number *He* = *0* and thus static friction occurs in the meshing, with the friction coefficient equal to the static coefficient $f = f_s$. As the Hersey number *He* increases (Figure 2), the value of the friction coefficient *f* decreases. The mating gear surfaces become partly separated. This type of friction is described by the mixed friction coefficient. A further increase in the Hersey number *He* causes the transition from mixed friction to fluid friction, with the friction coefficient reaching its minimum value $f = f_p$.

One method to achieve fluid friction between the worm thread and disc wheel tooth surfaces is to inject oil at sufficiently high pressure to separate the mating surfaces with an oil film. It should also be noted that under load, the surfaces of the worm thread and the disc wheel teeth may additionally deform.

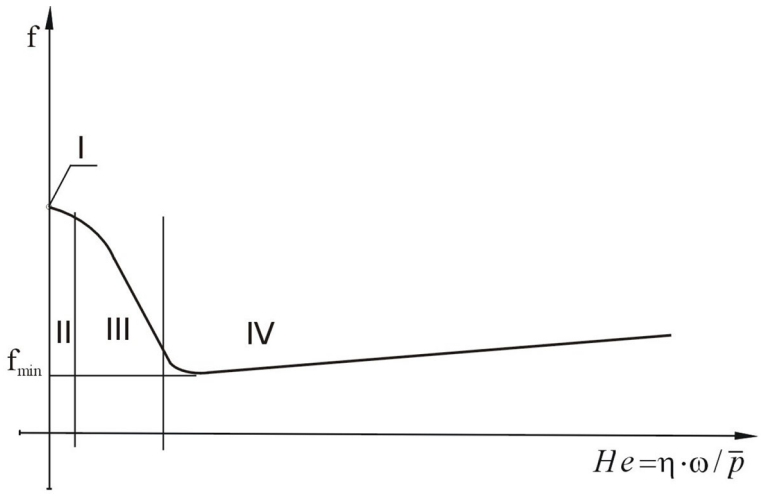


Figure 2. Types of friction: I – static friction, II – boundary friction zone, III – mixed friction zone, IV – fluid friction zone, He – Hersey number, h – dynamic viscosity of oil, w – angular velocity, $\overline{p}$ – average contact pressure

The formation of an elastohydrodynamic (EHD) oil film is influenced by the geometry of the contact surface, the strength properties of the materials used for the worm and the disc wheel, the thermophysical properties of the oil, the gear load as well as the gear ratio and the rotational speed at the input shaft. The formation of an EHD oil film allows the gear to operate with low friction.

The isothermal model developed by Dowson [13] is used to calculate the minimum oil film thickness. In this model, oil viscosity is specified at ambient temperature and pressure: T = T_0, p = p_0. However, gears operate at a temperature higher than ambient temperature. Therefore, to approximate the operating conditions obtained from numerical models to real-world conditions, correction factors are applied to calculate the oil film thickness, as mentioned earlier [14–16]. The correlation between the oil film thickness determined for the isothermal and non-isothermal models is obtained by introducing a correction factor C_{th}:

$$(h_{min})_{non\text{-}isothermal} = C_{th} \cdot (h_{min})_{isothermal} \tag{1}$$

where: C_{th} – correction factor for the minimum oil film thickness, h_{min} – the minimum oil film thickness.

The correction factor C_{th} presented in [13] depends on the thermal conductivity of the oil λ, the viscosity of the oil η_0 and the average velocity of the oil layers u. Its value is described by the following equation:

$$C_{th}(\xi) = \frac{1}{1 + 0{,}108 \cdot (\xi)^{0{,}62}} \tag{2}$$

where: $\xi = \dfrac{u^2 \cdot \beta \cdot \eta_0}{\lambda}$ – index of the influence of oil parameters on the minimum oil film thickness, β – coefficient of the influence of temperature on the dynamic viscosity of the oil, λ – thermal conductivity, $\eta_{(0)}$ – oil viscosity at ambient temperature, $u = (u_1 + u_2)/2$ – average linear flow velocity of the oil, u_1 – linear velocity of the worm thread, u_2 – linear velocity of the disc wheel tooth.

The value of the dimensionless coefficient is determined for the model of dynamic oil viscosity described by the equation developed by Crook [14]:

$$\eta(p,T) = \eta_0 \cdot e^{\alpha \cdot p - \beta (T - T_0)} \tag{3}$$

where: α – the piezo-coefficient of the effect of pressure on the dynamic viscosity of the oil (4), p – pressure in the oil film, ρ – coefficient of the effect of temperature on oil viscosity (5), T – temperature.

$$\alpha = \frac{1}{p} \cdot \ln \frac{\eta}{\eta_0} \tag{4}$$

$$\beta = \frac{\alpha \cdot p - \ln \dfrac{\eta}{\eta_0}}{T - T_0} \tag{5}$$

In engineering practice, other mathematical models are also used to calculate viscosity changes:

- The Barus model [14, 17]. The viscosity η_0 is determined at ambient temperature and ambient pressure $\eta = \eta_0(T = T_0, p = 0)$:

$$\eta = \eta_0 \cdot e^{\alpha \cdot p} \tag{6}$$

- The Rodermund model [14].

$$\ln \frac{\eta}{A} = \ln \frac{\eta_0}{A} \cdot \left(\frac{p}{2000} + 1 \right)^{D + E \cdot \ln \frac{\eta_0}{A}} \tag{7}$$

- The Witt model [14].

$$\eta = A \cdot e^{\frac{a_e - a_2 \cdot T}{a_1 + T}} \cdot e^{\left[(a_3 + a_4 \cdot p + a_{44} \cdot p^2) - \frac{T}{a_5 + a_6 \cdot p + a_{66} \cdot p^2} + a_7 + a_8 \cdot p + a_{88} \cdot p^2 \right] \cdot p} \tag{8}$$

where: A, D, E, α_p, a_3, a_4, a_{44}, a_7, a_8, a_{88}, – coefficients of the effect of pressure on dynamic viscosity, β_T, a_1, a_2, a_5, a_6, a_{66}, a_e, – coefficients of the effect of temperature on dynamic viscosity, p_0 – reference pressure, T_0 – reference temperature.

The values of the viscosity function $\eta = f(p,T)$ calculated based on the numerical model, when compared to the actual values determined experimentally, are subject to error. A comparison of various mathematical models and experimental results is presented in Figure 3 [14].

Given the differences between the dynamic viscosity values (η) calculated using numerical models and the measurement results (Figure 3), the authors decided to develop their own procedure for calculating the minimum oil film thickness, taking into account the effect of temperature on the dynamic viscosity of the oil. The

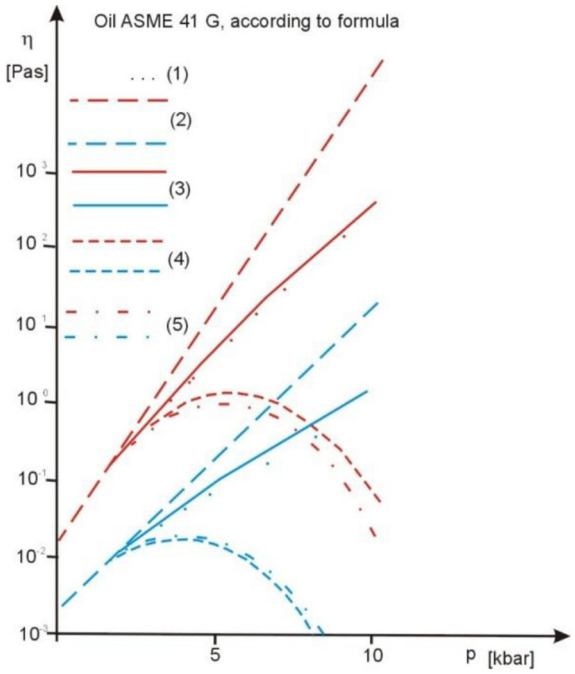


Figure 3. Comparison of mathematical models of viscosity as a function of pressure with experimental results: 1 – measurement results, 2 – the Barus model, 3 – the Rodermund model, 4 – the Crook model, 5 – the Witt model [14]

paper presents the results of calculations of the minimum oil film thickness in the meshing of the mating surfaces of the worm thread and the disc wheel tooth, considering the following oils: VG 32 and VG 150 [18].

KINEMATIC ANALYSIS OF A SPIROID GEAR

The profiles of the worm threads and the disc wheel teeth move relative to each other during gear operation. The parameters related to the motion of the meshing profiles significantly affect friction resistance, mechanical wear of the mating parts and oil temperature. A kinematic analysis of a spiroid gear, for which the distribution of instantaneous velocities at the meshing point C is shown in Figure 4, was performed in a Cartesian coordinate system, where x is the direction parallel to the longitudinal axis of the worm, z is the direction parallel to the longitudinal axis of the disc wheel and y is the direction perpendicular to the xy plane. The kinematic ratio of a spiroid gear is the quotient of the angular velocities of the worm and the disc wheel. For the gear in question, it is $i = \frac{\omega_1}{\omega_2} = 20$.

In the case of a spiroid gear, at the instantaneous meshing point C, the velocity tangent to the contact plane between the worm thread and the disc wheel tooth is the resultant velocity and is denoted by the symbol u in Figure 4. This velocity is opposite in direction to the friction force F_t. An analysis of the forces for a spiroid gear is presented in [16]. In the adopted x, y, z coordinate system, the components of the resultant velocity u are, respectively:

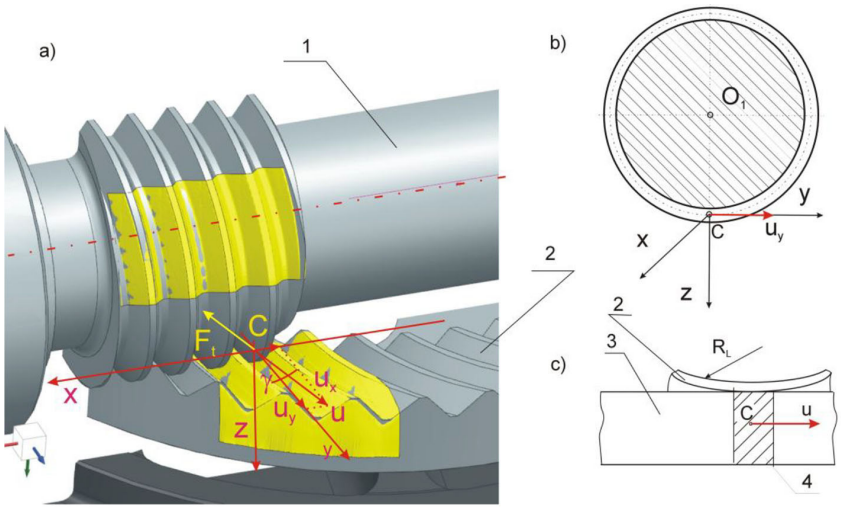


Figure 4. Kinematic analysis of a spiroid gear: a) velocity distribution at the meshing point of the worm thread and the disc wheel tooth, b) cross-section of the worm, c) contact trace between the disc wheel tooth and the worm thread. Symbols: 1 – worm, 2 – disc wheel, 3 – tangent plane to the contact trace between the disc wheel tooth and the worm thread, 4 – contact trace between the disc wheel tooth and the worm thread, R_l – radius of the disc wheel tooth line, F_t – friction force, x, y, z – reference axes, u – average oil flow velocity in the meshing of the worm and the disc wheel, γ – helix angle of the worm's thread line

$$u_x = u \cdot \sin\gamma,\ u_y = u \cdot \cos\gamma,\ u_z = 0 \qquad (9)$$

where: γ – helix angle of the worm's thread line.

Given that for the gear in question the helix angle of the worm's thread line is γ = 5°50, for further considerations, the linear velocity in the u_y coordinate direction can be taken as equal to the resultant velocity u:

$$u_y = u \cdot \cos 5^0 50' = u \cdot 0.9948 \approx \mathrm{u} \qquad (10)$$

THERMOPHYSICAL PROPERTIES OF THE ELASTOHYDRODYNAMIC OIL FILM

The isothermal model of an elastohydrodynamic oil film developed by Dowson [13] was constructed on the assumption that:

- the oil flow through the inter-tooth gap is laminar, steady and unidirectional in the direction of gap convergence (other directions of oil flow are negligible),
- the temperature of the oil film is constant,
- the effect of pressure on the viscosity and density of the oil is taken into account,
- the oil is a Newtonian fluid,
- the velocities of the oil boundary layer and the tooth surface are equal.

Taking the above into account, the isothermal oil film model can be described by the following equations:

- the distribution of oil pressure in the inter-tooth gap:

$$\frac{\partial}{\partial x}\left(\rho \cdot h^3 \frac{\partial p}{\partial x}\right) = 12 \cdot \frac{\partial(h \cdot \rho)}{\partial x} \cdot \frac{u_1 + u_2}{2} \qquad (11)$$

- the normal stress state in the contact zone between the worm thread and the disc wheel tooth:

$$\sigma_H(x) = \frac{\sigma_{H\max}}{a}\sqrt{a^2 - x^2},\ gdzie\ -a \le x \le a \qquad (12)$$

- the shape of the gap in the zone where the worm thread and the disc wheel tooth do not undergo deformation:

$$h(x) = h_0 + \frac{x^2}{2 \cdot R_L} \qquad (13)$$

oil viscosity and density $\eta = f(p, T = const)$, $\rho = f(p, T = const)$ described by the Barus Equation 6. Solving the above system of equations (11–13) enables calculation of the minimum oil film thickness [13, 19]:

$$h_{\min} = 2.65 \cdot (\eta_0 \cdot u)^{0.7} \cdot \alpha^{0.54} \cdot E'^{0.03} \cdot R_L^{0.43} \cdot \left(\frac{F_n}{b}\right)^{-0.13} \qquad (14)$$

where: $\frac{1}{E'} = \frac{1}{2} \cdot \left(\frac{1-\nu_1^2}{E_1} + \frac{1-\nu_2^2}{E_2}\right)$, $\frac{1}{R_L} = \frac{1}{R_L} + \frac{1}{\infty}$, R_L – radius of the disc wheel tooth line, h – a flat worm thread profile was assumed.

By introducing dimensionless factors: UZ – oil flow velocity factor, M – material factor and G – load factor:

$$UZ = \frac{\eta_0 \cdot u}{E' \cdot R_L},\ M = \alpha \cdot E',\ G = \frac{F_{nb}}{E' \cdot R_L},\ F_{nb} = \frac{F_n}{b} \qquad (15)$$

Equation 1 was brought to dimensionless form:

$$H^*_{\min} = \frac{h_{\min}}{R_L} = 2.65 \cdot UZ^{0.7} \cdot M^{0.54} \cdot G^{-0.13} \qquad (16)$$

A necessary condition for fluid friction is that hydrodynamic lift forces generate an inter-tooth gap height satisfying the following condition, which can be expressed in two forms:

- dimensional:

$$h_{\min} \ge h_{\lim} = 1.1 \cdot (R_{z1} + R_{z2}) \qquad (17)$$

- dimensionless:

$$H_{b\min} \ge H_{b\lim} = \frac{1.1 \cdot (R_{z1} + R_{z2})}{\rho_z} \qquad (18)$$

where: R_{z1} and R_{z2} denote the surface roughness of the worm thread and the disc wheel tooth, respectively.

The coefficients of the influence of pressure and temperature on the dynamic viscosity of the oil are determined from the oil characteristics obtained experimentally $\eta = f(p, T = const)$. Knowledge of oil characteristics enables their use in Dowson's isothermal model (14) and the determination of the minimum oil film thickness (EHD) without applying the discussed correction factor C_{th}.

The authors of publication [18] conducted measurements of the viscosity η *(p, T)* for VG 32 and VG 150 oils in accordance with the methodology described. Their test results, for fixed oil temperatures of T = 40, 60, 90, 120 °C, are presented in the graphs in Figures 5 and 6.

The graphs in Figures 5 and 6 clearly show that as pressure p increases, the dynamic viscosity of the oil η increases.

To determine the dimensionless coefficients (15) for VG 32 and VG 150 oils, based on the oil characteristics (Figures 5 and 6) and the Barus model (6), the values of dynamic viscosity η_0 and the values of the piezo-coefficient α ($T = const$) were determined (Tables 1 and 2).

The calculations show that the higher the VG oil grade, the higher its dynamic viscosity, and the lower the value α.

Upon analyzing Equations 15 and 16, it can be observed that the minimum oil film thickness H_{bmin} is significantly influenced by the following factors, due to the values of the power exponent of the oil flow velocity factor $UZ^{0.7}$ and the material factor $M^{0.54}$: η_0 – oil viscosity, α – oil piezo-coefficient

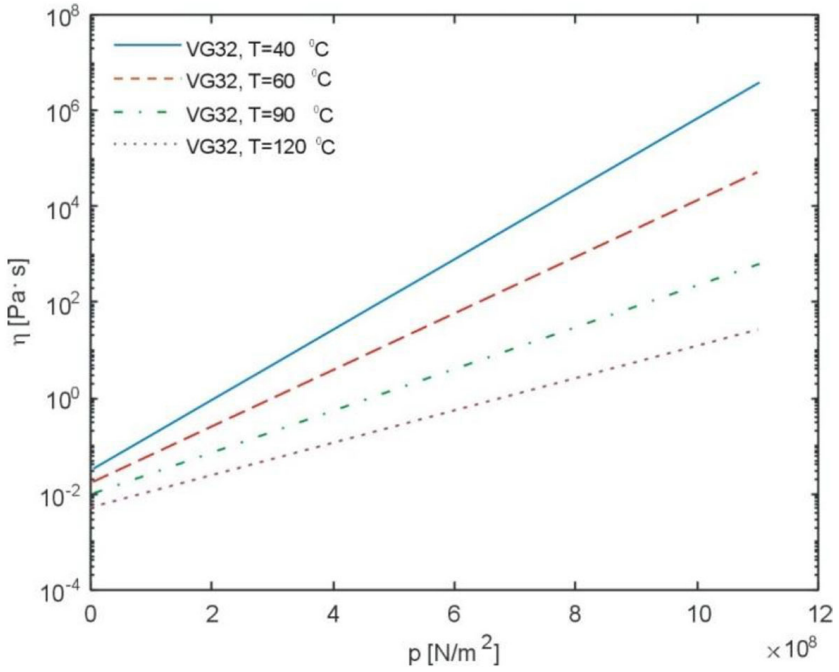


Figure 5. Effect of oil pressure on the dynamic viscosity of VG 32 oil

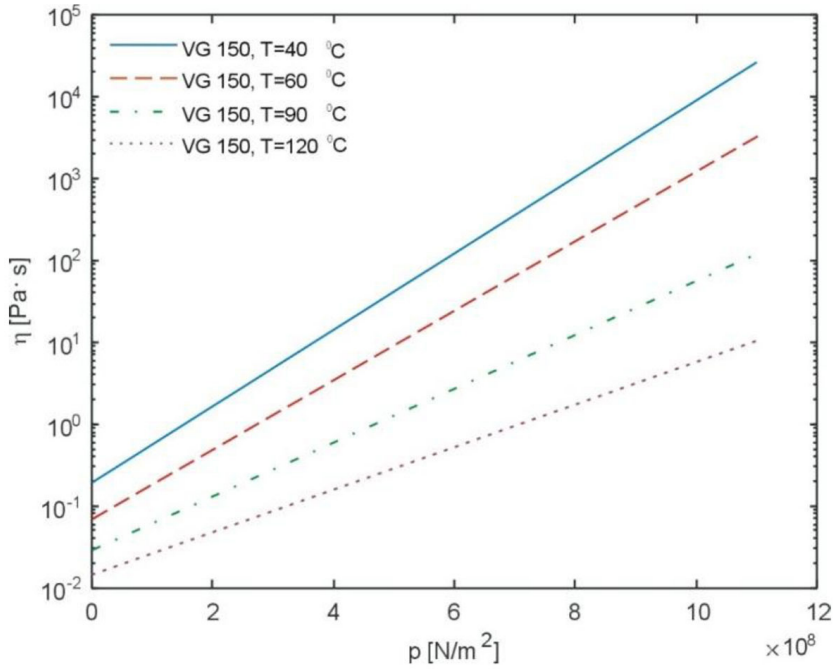


Figure 6. Effect of oil pressure on the dynamic viscosity of VG 150 oil

Table 1. Dynamic viscosity η_0 of VG 32 and VG 150 oils

Oil class	Oil temperature T [°C]			
	40	60	90	120
	Dynamic viscosity of the oil η *(p = 0)* = η_0 [Pa·s]			
VG 32	2.992H10^{-2}	1.664H10^{-2}	0.956H10^{-2}	0.501H10^{-2}
VG 150	18.640H10^{-2}	6.600H10^{-2}	2.830H10^{-2}	1.410H10^{-2}

Table 2. Values of the piezo-coefficient (α) for VG 32 and VG 150 oils

Oil class	Oil temperature T [°C]			
	40	60	90	120
	Piezo-coefficient of the oil α [1/Pa]			
VG 32	1.699H10^{-8}	1.358H10^{-8}	1.012H10^{-8}	0.786H10^{-8}
VG 150	1.080H10^{-8}	0.984H10^{-8}	0.760H10^{-8}	0.600H10^{-8}

and $u = (u_1 + u_2)/2$ – the average oil flow velocity in the inter-tooth gap. In turn, the value of the power exponent at the load factor $G^{-0.13}$ indicates its smaller contribution to the formation of an oil film in the inter-tooth gap that satisfies the condition $H_{b\min} \geq H_{b\lim}$. In preliminary gear design calculations, the oil and its physical properties are assumed, including: η, ρ. In the next stage of calculations, however, it is verified, taking into account the actual operating conditions of the gear, whether the condition for fluid friction is met. To perform gear design calculations, the following must be known:

- E_1, E_2 – Young's modulus of the material for the mating toothed rims of the worm and the disc wheel,
- F_n – concentrated load, relative to a single tooth of the disc wheel,
- n_1 – rotational speed of the worm,
- R_L – radius of the disc wheel tooth line,
- η_0, a – thermophysical properties of the oil η_0, α,
- T – oil temperature in the meshing area.

CALCULATION OF THE EHD PROPERTIES OF THE OIL FILM IN THE MESHING OF THE DISC WHEEL AND THE WORM THREAD

The oil film properties were calculated using the following input values:

- load F_n = 1000 and 3000 N,
- thermophysical properties of the oils discussed in section 3,
- average oil flow velocities in the meshing of the worm and the disc wheel u = 2.45, 4.9, 7.35 m/s,
- oil temperatures in the meshing of the worm and the disc wheel T = 40, 60, 90, 120 °C.

The following dimensionless values were sought as output quantities:

- factors UZ, M, G,
- minimum oil film thickness H^*_{min}.

The test results for the load F_n = 3000 N and factor G = 3.474 are presented in the graphs (Figures 7 and 8). The results of calculations for the velocity u = 7.35 m/s and load F_n = 1000, 3000 N are presented in the graphs (Figures 9–11).

The product of oil viscosity and oil flow velocity $\eta_0 \cdot u$ has a significant influence on the fulfillment of the condition guaranteeing fluid friction, i.e. $H_{b\min} \geq H_{b\lim}$. The study considered oils of two grades, VG 32 and VG 150, with significantly different viscosities. With the increase of the product $\eta_0 \cdot u$, the values of the M and UZ factors and the minimum oil film thickness H^*_{min} increase (Figures 7, 8). For VG 32 oil, an increase in velocity to u = 7.35 m/s cannot guarantee fluid friction. In contrast, VG 150 oil at velocities u > 4.90 m/s and oil temperatures T < 60 °C can ensure fluid friction. For oil temperature T = 40 °C, an increase in oil velocity from u = 4.90 m/s to u = 7.35 m/s resulted in a 50% increase in the minimum oil film thickness: from $H^*_{\min} = 5.57 \cdot 10^{-5}$ to $H^*_{\min} = 8.35 \cdot 10^{-5}$.

The results of calculations for the velocity u = 7.35 = const m/s and the loads F_n = 1000 and 3000 N are presented in Figures 9–11.

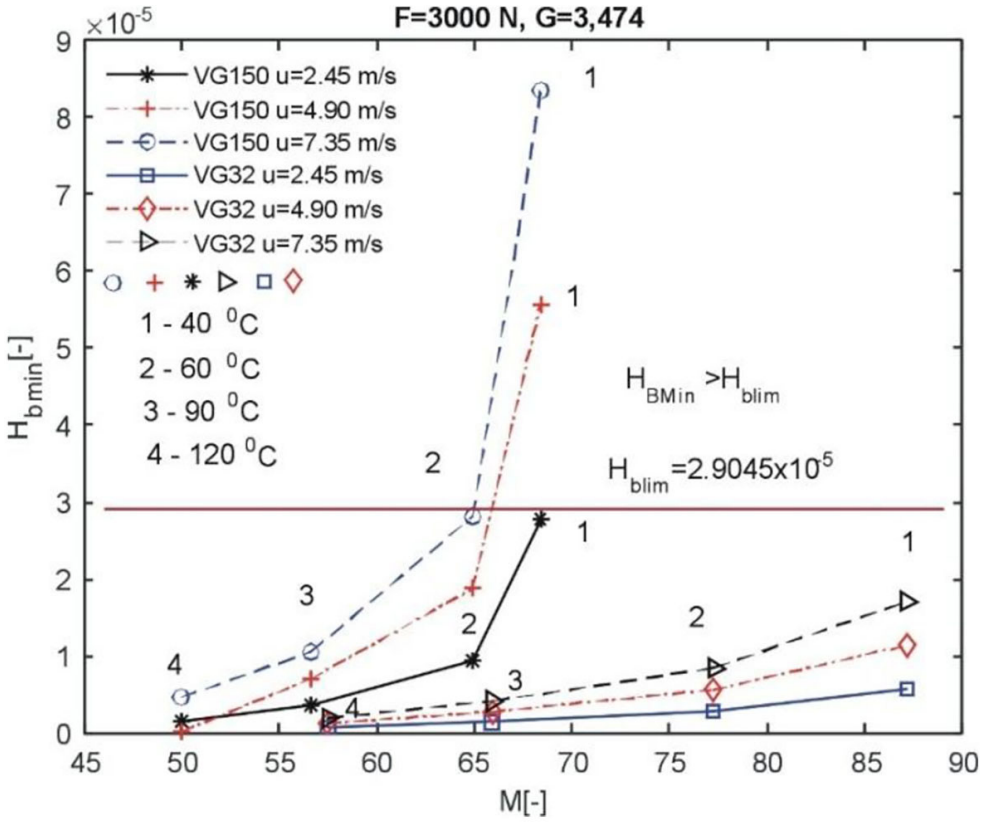


Figure 7. Effect of the material factor M, measured at a constant load F_n = const, on the minimum oil film thickness $\mathbf{H_{bmin}}$

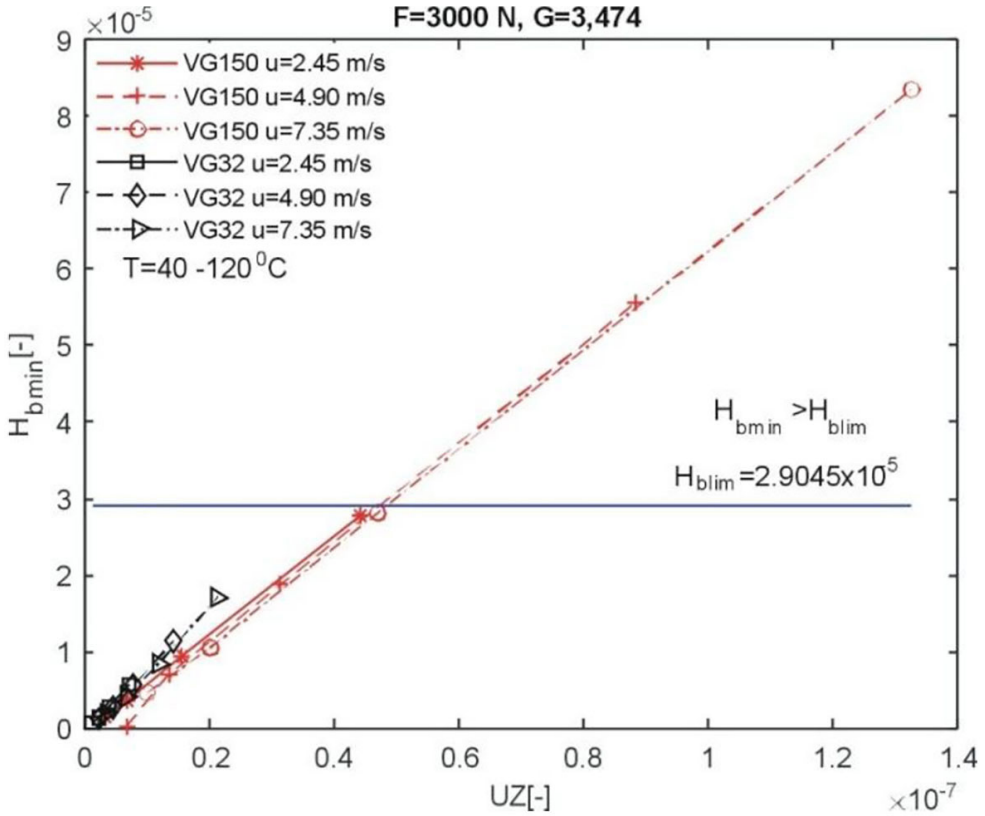


Figure 8. Effect of the oil flow velocity factor UZ, measured at a constant load F_n = const, on the minimum oil film thickness H_{bmin}. Temperature values T = 40, 60, 90, 120 °C correspond to points 1, 2, 3, 4 in Figure 7

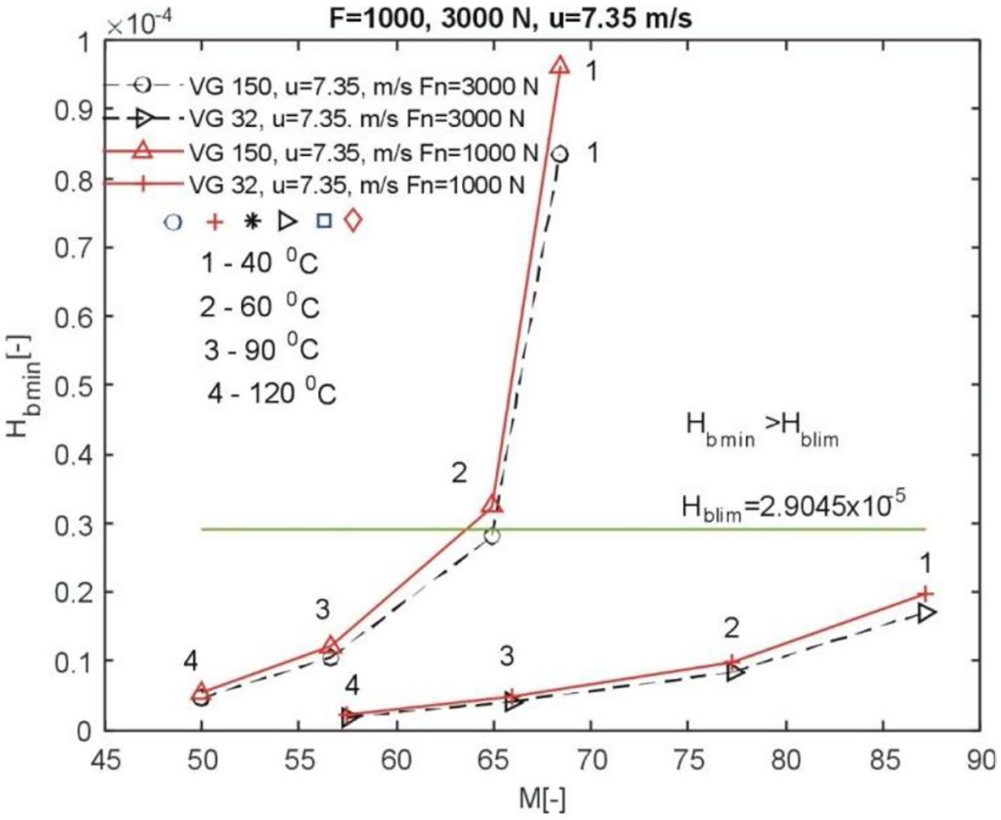


Figure 9. Effect of the material factor M, measured at a constant oil velocity u = const, on the minimum oil film thickness H_{bmin}

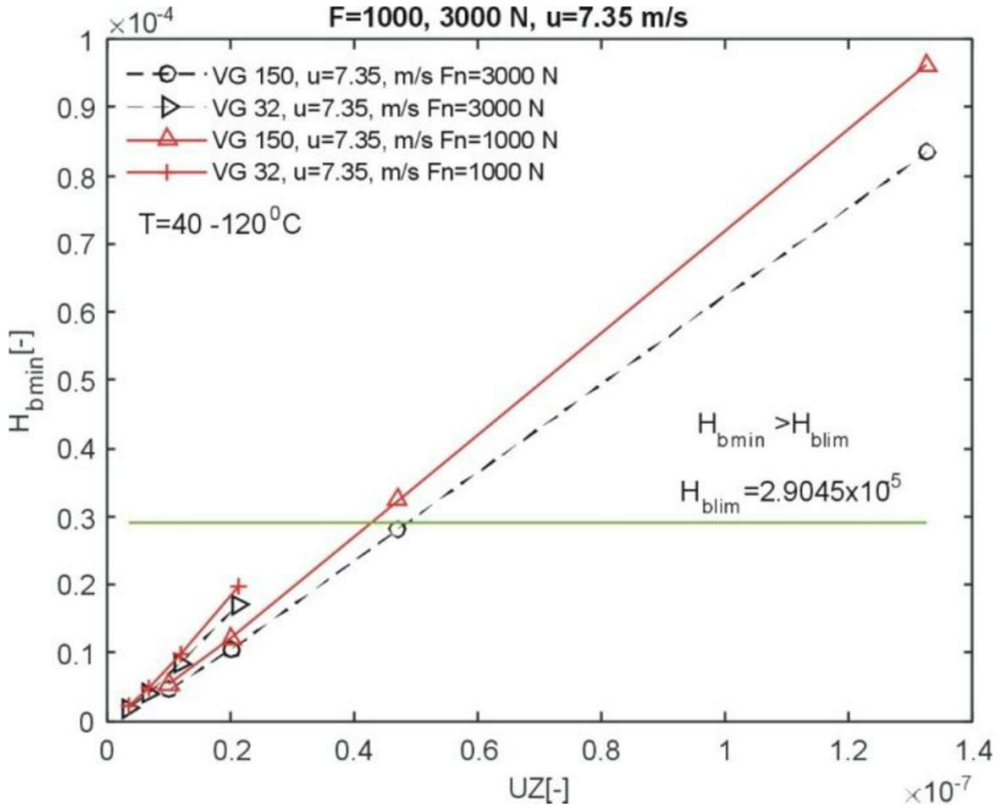


Figure 10. Effect of the oil flow velocity factor UZ, measured at the constant oil velocity u = const, on the minimum oil film thickness H_{bmin}

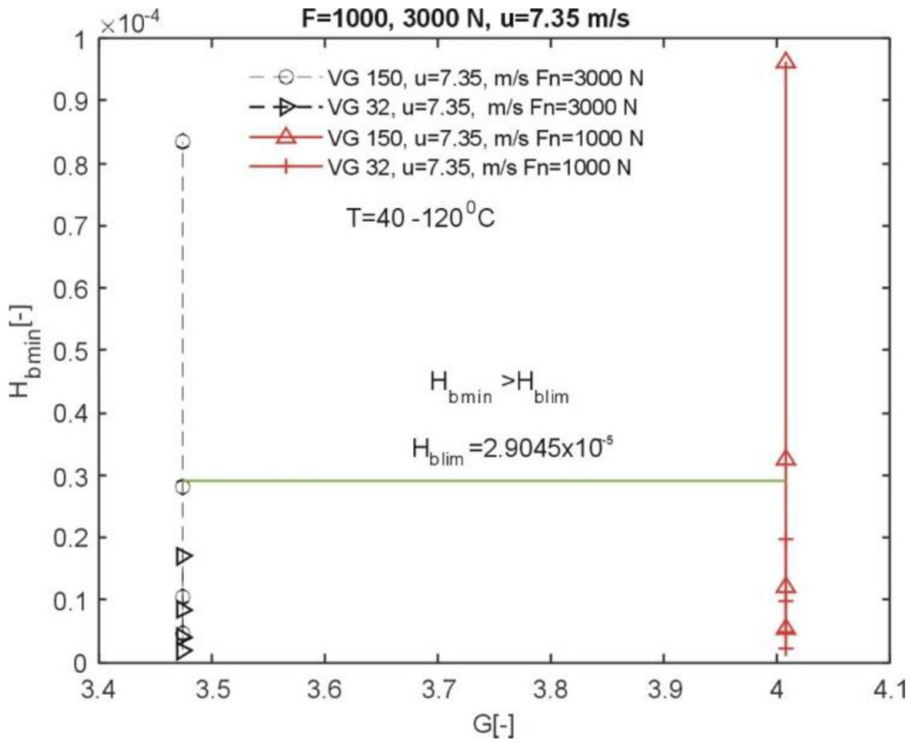


Figure 11. Effect of the load factor *G*, measured at a constant oil velocity *u* = const, on the minimum oil film height H_{bmin}. Temperature values T = 40, 60, 90, 120 °C correspond to points 1, 2, 3, 4 in Figure 9

The temperature values T = 40, 60, 90, 120 °C correspond to points 1, 2, 3, 4 in Figure 9. By analyzing the graphs of the functions $UZ(H_{bmin})$, $M(H_{bmin})$ and $G(H_{bmin})$ shown in Figures 9–11, it can be observed that the values of the minimum oil film thickness $H_{(bmin)}$ increase along with an increase in the factors *UZ, M,* and *G.* The condition for proper gear operation, i.e. $H_{b\min} \geq H_{b\lim}$, is satisfied for the load F_n = 3000 and 1000 N for VG150 oil and oil temperature T < 60 °C. An increase in load results in a decrease in the minimum oil film thickness. Thus, for oil temperature T = 40 °C, an increase in load from F_n = 1000 N to F_n = 3000 N caused a 13% decrease in the minimum oil film thickness from $H_{bmin} = 9.63 \cdot 10^{-5}$ to $H_{bmin} = 8.35 \cdot 10^{-5}$.

CONCLUSIONS

The minimum oil film thickness required for the operation of a spiroid gear with fluid friction is significantly influenced by the product of the average oil flow velocity through the inter-tooth gap and the dynamic viscosity of the oil $(u_0 \cdot \eta_0)$ as well as the value of the oil's piezo-coefficient α. As the test results showed, the gear should be lubricated with oil of viscosity appropriately selected for the operating conditions. Lubricating the gear with oils of too low viscosity, especially when operating at low rotational speeds and under high loads, can lead to operation in the mixed friction range. As the bench tests have shown, oil temperature is a significant parameter that also affects the properties of the oil film.

Unlike the classical gear design method, where the ambient temperature is a given parameter and the thickness of the non-isothermal oil film is corrected by an appropriate temperature coefficient, in the proposed method, calculations of the minimum oil film thickness take into account the actual temperature occurring in the meshing of the disc wheel and the worm thread during operation.

The developed methodology significantly simplifies the process of calculating non-isothermal models of the elastohydrodynamic oil film. According to the authors, due to the use of experimentally determined viscosity functions $\eta(T, p)$ and oil density functions $\rho(T, p)$, the presented method enables a better approximation of the gear's operating parameters to its actual operating conditions.

By using dimensionless factors, i.e. the material factor *M*, the load factor *G* and the oil flow velocity factor UZ, the calculation results can be generalized to develop performance

characteristics for certain series of design solutions. These characteristics can also be used in the process of designing other gear types.

By analyzing the material factor M and the oil flow velocity factor UZ, it can be observed that reducing the radius of the disc wheel tooth line $R_{(L)}$ allows for an increase in the minimum oil film thickness H^*_{min}.

REFERENCES

1. Goldfarb V., Trubachev E., Barmina N. Innovations in design and production of spiroid gears in the 21st century. In: MATEC Web of Conferences. Power transmissions, 2019; 287, 01002.
2. Davall website. https://www.davall.co.uk/
3. Spiroid website. https://www.spiroidgearing.com/application-industries
4. Trubachev E. Spiroid gears as an alternative to bevel and hypoid gears. In: Proceedings of the 9th International Conference on Industrial Engineering (ICIE 2023) 2023; 71–82.
5. Abadjiev V., Abadjieva E. On an approach to the synthesis, design, and manufacture of hyperboloid gear sets with face-mating gears. Part 1: Basic theoretical and CAD experience. Journal of Theoretical and Applied Mechanics 2016; 46(2), 3–26.
6. Litvin F. L., Nava A., Qi Fan, Fuentes A. New geometry of worm face gear drives with conical and cylindrical worms: Generation, simulation of meshing, and stress analysis. NASA/CR—2002-211895 ARL–CR–0511 U.S. Army Research Laboratory. University of Illinois at Chicago, Chicago, Illinois November 2002.
7. Evertz F., Gangireddy M., Mork B., Porter T., Quist A. High torque skew axis gearing. Spiroid high torque skew axis gearing, 2023.
8. Żabicki M. Gearbox Diagnostics—Diagnostics, Measurements, Regulation, Chief Mechanic. January–February 2020.
9. Frąckowiak P., Meshing trace in a flat spiroidal gear. Archives of Machine Technology and Automation 2009; 19(4), 59–71.
10. Spałek J., Kwaśny M. Diagnostic verification of the influence of lubricating oil viscosity on gear transmission operation. High-Speed Tracked Vehicles 2012; 29(1).
11. Chodoła Ł., Mazurkow A., Surowaniec M., Markowski T., Homik W.: Measurement method of temperature of the face gear rim of a spiroid gear. Sensor: An Open Access Journal 2022; 22(22).
12. Mazurkow A., Homik W., Chodoła Ł., Pacana J., Lewicki W. Measurement and numerical method for determining the contact position of gear rims in a spiroid gearbox. Advances in Science and Technology Research Journal, 2026.
13. Dowson D., Higginson G.R. A numerical solution to the Elasto-Hydrodynamic Problem. J. Mech. Engng. Sci. 1959; 1, 6–15.
14. Haddad, N. Viscosity and Friction Measurements in EHD Line Contact. Dissertation, TU Hannover, 1985.
15. Ghos M.K., Hamerock B.J. NASA Technical Memorandum 1983; 83424.
16. Mazurkow A., Homik W. Studies of selected tribological characteristics of spiroid gears in the context of the molecular-mechanical theory of friction. Transport Problems, 2025; 1.
17. Barus C. Isotherms, isopyests, and isometrics relative to viscosity. American Journal of Science 1993; 45, 87–96.
18. Belicke R, Bobach L., Bader N., Poll G., Brouwer L., Schwarze H. Tribological fluid models for simulating friction in lubricated concentrated contacts. In: Tribology – Symposium, Society for Tribology e.V. Göttingen, 2015.
19. Krzemiński-Freda H. Pressure distribution and shape of the oil film in elastohydrodynamically lubricated rolling elements. Doctoral dissertation. 1969. Łódź.